Effects of x-ray irradiation on polycrystalline silicon, thin-film transistors

Yixin Li, Larry E. Antonuk,[a] Youcef El-Mohri, Qihua Zhao, Hong Du, Amit Sawant, and Yi Wang

Department of Radiation Oncology, University of Michigan, 519 West William Street, Ann Arbor, Michigan 48103-4943

The effects of x-ray irradiation on the transfer and noise characteristics of excimer-laser-annealed polycrystalline silicon (poly-Si) thin-film transistors (TFTs) have been examined at dose levels up to 1000 Gy. Parameters including mobility, threshold voltage, subthreshold swing, and leakage current, as well as flicker and thermal noise coefficients, were determined as a function of dose. In addition, the physical mechanisms of the observed changes in these parameters are analyzed in terms of radiation-generated charge in the gate oxide, at the $Si-SiO_2$ interface, and at the grain boundaries. The results of the studies indicate that poly-Si TFTs exhibit sufficient radiation tolerance for the use in active-matrix flat-panel imagers for most medical x-ray applications. © *2006 American Institute of Physics.* [DOI: 10.1063/1.2179149]

I. INTRODUCTION

Over the past three decades, polycrystalline silicon (poly-Si) has played an increasingly important role in a broad range of semiconductor-related technologies.[1] For example, it is widely used in integrated circuits such as dynamic and static random-access memories,[1–4] in microelectromechanical systems,[5] in solar cells,[6] and in large-area electronic systems such as flat-panel active-matrix displays.[1,7] The tremendous interest in poly-Si has been due, in part, to the fact that this material exhibits high carrier mobilities (on the order of 100 cm^2/V s for both electrons and holes),[8] and lends itself toward inexpensive and large-area deposition.[9]

These characteristics of poly-Si make it a promising candidate for the use in the emerging technology of active-matrix flat-panel imagers (AMFPIs).[10] AMFPIs are digital x-ray imaging devices that incorporate a two-dimensional array of imaging pixels, each pixel consisting of an amorphous silicon (*a*-Si) thin-film transistor (TFT) coupled to other pixel components which convert incident x-ray radiation to charge and store this imaging signal in the pixel.[11] Such imagers have demonstrated levels of performance equivalent, or superior to those exhibited by traditional, non-digital imaging technologies, as well as offering many other advantages.[10] Consequently, AMFPIs are being rapidly integrated into a wide variety of medical and industrial imaging applications.[11]

However, under certain circumstances, such as fluoroscopic imaging performed at low doses and mammographic imaging at high spatial resolution, the performance, as characterized by the signal-to-noise ratio (SNR), of present-day AMFPIs is significantly constrained.[12,13] One promising approach for overcoming such limitations is to enhance the SNR by incorporating in-pixel amplifiers into the array designs.[10,12,14,15] While *a*-Si TFTs are well suited to their role as pixel switches, challenges exist in configuring them as

amplifiers with sufficient performance.[16] For this reason, poly-Si fabricated by excimer laser annealing[8] (ELA) is being investigated as a possible alternative for *a*-Si, and several prototype AMPFI designs based on poly-Si TFTs have been reported.[14,17,18] In addition, the use of poly-Si opens up other possibilities, such as the achievement of considerably higher frame rates as well as the incorporation of peripheral circuits (e.g., data-line multiplexers and gate-line drivers) on the array substrate in order to reduce the need for external electronics and thus lower manufacturing costs.[19]

An important consideration for x-ray imaging devices is that they are exposed to large amounts of ionizing radiation during their operational lifetime. For example, the estimated average dose per year for an AMFPI in diagnostic x-ray imaging applications is ~2 Gy in fluoroscopy,[20,21] ~10 Gy in chest radiography,[21,22] and ~50 Gy in mammography[23] while it is ~500 Gy in megavoltage radiotherapy imaging.[24] With an imaging equipment typically expected to last at least 5 years, it is therefore critical that poly-Si circuit elements be able to tolerate correspondingly high radiation levels.

The effects of radiation of various types of solid-phase crystallized (SPC) poly-Si TFTs at a single dose (equivalent to ~10 000 Gy) has been reported in an earlier study by Yang *et al.*[25] However, poly-Si TFTs fabricated by ELA, the presently preferred method,[9,26] exhibit significantly different structure (i.e., much larger grain size) and better properties (e.g., higher mobility and sharper turn on). It is therefore interesting to examine the radiation-induced effects on ELA poly-Si TFTs, which are critical to the above-mentioned applications, but are still largely unknown. In this work, we systematically examine various properties of ELA poly-Si TFTs, including mobility, threshold voltage, subthreshold swing, leakage current, and thermal and flicker noise amplitudes, as a function of dose up to 1000 Gy. In addition, the physical mechanisms underlying these effects are discussed in terms of the change in trapped charge in the gate oxide, at the $Si-SiO_2$ interface and at the poly-Si grain boundaries.
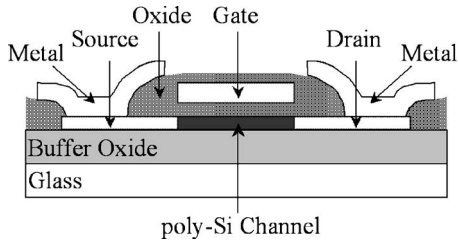
[a] Electronic mail: antonuk@umich.edu

FIG. 1. Schematic drawing of the cross section of the type of polycrystalline silicon TFTs examined in this study (not to scale), adapted from Ref. 8. The TFTs have a single gate structure and the poly-Si channel and the gate oxide are about 50 and 100 nm thick, respectively.

Finally, the implications of the observed effects with respect to medical applications requiring different lifetime levels of doses are discussed.

II. EXPERIMENTAL DETAILS

The ELA poly-Si TFTs used in this study were produced at the Palo Alto Research Center (PARC). A schematic diagram illustrating the structure of these TFTs is shown in Fig. 1. All the TFTs examined in the present study are n type, with channel widths (W) ranging from 5 to 50 μm and channel lengths (L) ranging from 10 to 50 μm, as listed in Table I.

All the TFTs used in the study were fabricated on the same test chip. To allow an accurate determination of dose, the test chip was placed in an acrylic enclosure, with 2.7 cm of overlying material serving as dose buildup layer and 10 cm of underlying material serving to provide full backscatter. The enclosure is attached to the accessory mount of a Varian 21EX linear accelerator. With this configuration, the TFTs were irradiated by a 6 MV therapy beam at a dose rate of 0.04 Gy/s. (Note that the dose values reported in this paper correspond to dose to water at the position of the test chip, using the known calibration of the linear accelerator.) The radiation was delivered in steps ranging from 10 to 200 Gy per step, up to a total dose of 1000 Gy, with measurements performed after each step. This cumulative dose significantly exceeds the lifetime dose received by diagnostic x-ray imagers and the yearly dose for megavoltage imagers. During the irradiations, no bias voltage was applied to the TFTs. After each irradiation step, current-voltage and

TABLE I. Specifications of the width (W) and length (L) parameters of the poly-Si TFTs examined in this study.

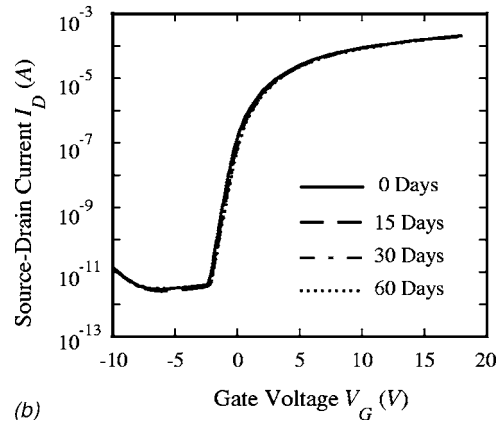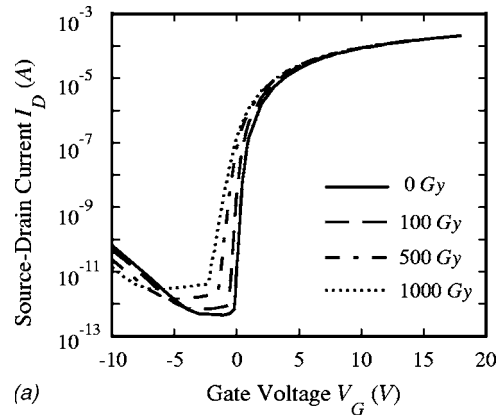| Channel width W (μm)	Channel length L (μm)
5	50
10	50
5	15
10	15
10	10
50	50
50	15
50	10

FIG. 2. Transfer characteristics obtained from a poly-Si TFT with $W=L$ $=50$ μm, under a source-drain voltage of 5 V. The measurements were performed (a) prior to the first irradiation and after receiving 100, 500, and 1000 Gy and (b) immediately after receiving 1000 Gy, as well as 15, 30, and 60 days later.

noise characteristics were measured for each of the TFTs, and the results are presented in the following section as a function of cumulative dose.

III. RESULTS

Figure 2(a) shows an example of the effects of x-ray irradiation on the transfer characteristics of a representative poly-Si TFT before irradiation and after receiving 100, 500, and 1000 Gy. As dose increases, the subthreshold region is seen to shift toward more negative gate voltages and becomes shallower. This indicates an increase in the subthreshold swing S and a change in the threshold voltage V_T. For gate voltages V_G, where the TFT is fully conducting ($V_G > 5$ V), the curves for the various doses overlap, indicating that there is no significant degradation in TFT mobility. Finally, in the nonconducting region of the TFT ($V_G < 0$ V), an apparent increase in the leakage current is observed. Figure 2(b) shows transfer characteristics measured up to 60 days following the final irradiation, during which the TFT was kept at room temperature ($\sim$295 K). All the curves in Fig. 2(b) largely overlap, which suggests the absence of any room-temperature annealing effects over this period.
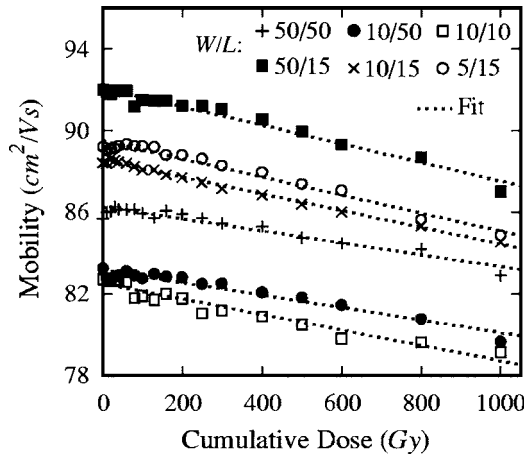
FIG. 3. Mobility of poly-Si TFTs, as a function of dose, along with fits using Eq. (3). For reasons of clarity, data for two other TFTs, which overlap with the presented ones, are not shown. These results, and those in Figs. 4–6, were obtained from data such as that shown in Fig. 2.

A. Effects on mobility

In general, for sufficiently high positive gate voltages (for example, $V_G > 10$ V) and small drain voltages V_D (i.e., $V_D < V_G - V_T$) the source-drain current I_D of thin-film transistors exhibits a linear dependence on V_G,[27,28]

$$I_D = \mu C_{ox}(W/L)(V_G - V_T - V_D/2)V_D, \qquad (1)$$

where μ is the TFT mobility, C_{ox} is the gate oxide capacitance per unit area, and V_T is the threshold voltage. For each measured transfer characteristic curve, μ and V_T were determined from the slope and the intercept, respectively, of a linear fit of Eq. (1) to the portion of the data corresponding to gate voltages greater than 10 V. Note that the overall uncertainty in the measurements of the source-drain current under these gate voltages was less than 0.1%, and the uncertainty in the values of applied voltage was less than 1 mV. As a result, the error in the determination of μ and V_T is estimated to be less than 0.15% and 0.02 V, respectively.

Figure 3 shows the mobility μ of the TFTs as a function of dose. As seen in the figure, after 250 Gy (which corresponds to the approximate dose a mammographic imager receives over 5 years), the degradation of the mobility is less than 1%. This change is fairly minor and thus the operation of AMFPIs with poly-Si TFTs for diagnostic applications should not be significantly affected. In addition, after receiving the total 1000 Gy (which corresponds to approximately two years of use for a megavoltage radiotherapy imager), the degradation is still only about 4%–5%.

In order to interpret the observed degradation in the mobility of the poly-Si TFTs, we note that the mobility degradation of crystalline silicon (c-Si) metal-oxide semiconductor field-effect transistors (MOSFETs) has been reported to follow the expression:

$$\mu = \frac{\mu_0}{1 + \eta \Delta N_{it}}, \qquad (2)$$

where μ_0 is the mobility prior to irradiation, ΔN_{it} is the radiation-induced increase in the aerial density of trapping states at the Si–SiO$_2$ interface of the transistor, and η is a

constant which has been measured to be $7 \pm 1.3 \times 10^{-13}$ cm^2.[29] For the poly-Si TFTs, an expression with a similar form to that of Eq. (2) was used to examine the relationship between the measured values of μ and the absorbed dose D,

$$\mu = \frac{\mu_0}{1 + \gamma D}, \qquad (3)$$

where γ is a constant. From a fit of Eq. (3) to the data shown in Fig. 3, an average value for γ of $4.4 \pm 0.6 \times 10^{-5}$ Gy^{-1} is obtained. With the assumption that Eq. (2) also applies to poly-Si TFTs, a relationship between ΔN_{it} and the absorbed dose D can be obtained by combining Eqs. (2) and (3),

$$\Delta N_{it} = \frac{\gamma}{\eta} D, \qquad (4)$$

The linear dependence of ΔN_{it} on dose for poly-Si TFTs indicated by this equation is similar to what has been modeled[30,31] and observed[32–34] in c-Si MOSFETs at dose levels comparable to those of the present study. Equation (4) is used in the analysis of radiation-induced effects on the threshold voltage and subthreshold swing in the following sections. [Note that the assumption of the applicability of Eq. (2) to poly-Si TFTs implies that the mobility degradation of such TFTs is due to an increase in the density of trapping states at the Si–SiO$_2$ interface, as is the case for c-Si MOSFETs.]

B. Effects on threshold voltage

The threshold voltage as a function of dose is plotted in Fig. 4(a). For all poly-Si TFTs examined, V_T is seen to decrease by ~ 1 V in the first 500 Gy, then increase very slowly with further dose. Given that the voltages used to render TFTs conducting and nonconducting on imaging arrays are typically ~ 15 and -5 V, respectively, the observed shift in V_T should not significantly affect the addressing of AMFPI pixels. For AMFPI arrays with in-pixel amplifiers employing a source-follower circuit,[18] this shift may induce an offset in imaging signal (which is in proportion to [$V_G - V_T$]—but such an offset should not pose a problem since it can be corrected through gain and offset corrections of the type that are routinely used in postprocessing of image frames.[35]

As in the case of c-Si MOSFETs, the observed shift in threshold voltage for the poly-Si TFTs ΔV_T can be separated into contributions due to the charge trapped at the Si–SiO$_2$ interface ΔV_{it} and in the gate oxide ΔV_{ot},[36,37]

$$\Delta V_T = \Delta V_{it} + \Delta V_{ot}. \qquad (5)$$

For the TFTs used in this study, which are all n type, the radiation-generated interface trapping states are generally acceptorlike and hence charged with electrons after band bending. This leads to a positive ΔV_{it}, since a higher threshold voltage is needed to compensate for the trapped electrons,

$$\Delta V_{it} = q \Delta N_{it}/C_{ox}, \qquad (6)$$

where q is the electron charge. On the other hand, ΔV_{ot} is generally negative for n-type TFTs, since the electric field

FIG. 5. Subthreshold swing S as a function of dose for each of the poly-Si TFTs.
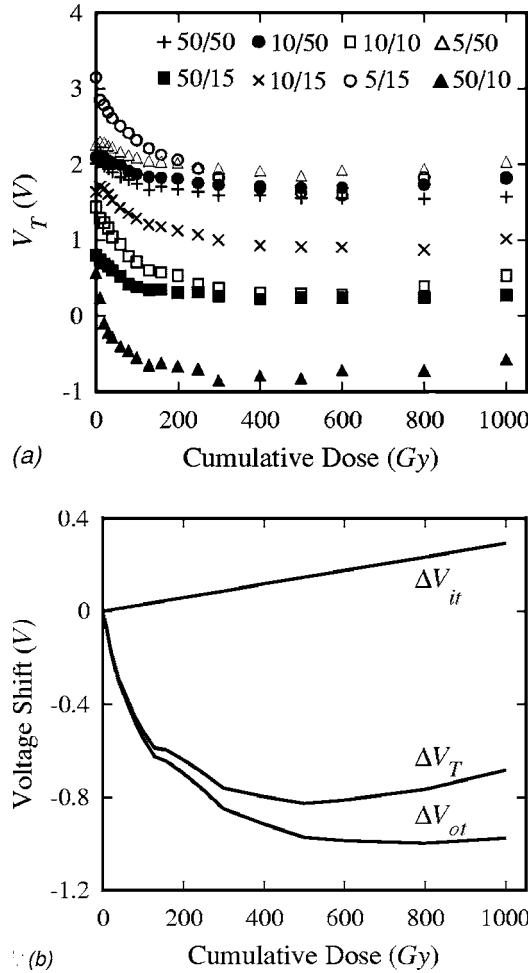

FIG. 4. (a) Threshold voltage V_T as a function of dose for each of the poly-Si TFTs. (b) Change in threshold voltage ΔV_T averaged over the eight TFTs. This change is separated into two components: a change due to electrons trapped at Si–SiO$_2$ interface ΔV_{it} and a change due to holes trapped in the gate oxide ΔV_{ot}.

C. Effects on subthreshold swing

Another important property of the poly-Si TFTs, the subthreshold swing S, was determined from the inverse of the maximum slope $(\partial V_G / \partial \log_{10} I_D)$ of the transfer characteristic curves in the subthreshold region. In this region, the uncertainty in the measurement of the source-drain current is less than 1%. As seen in Fig. 5, the resulting values for S exhibit an approximately linear dependence on dose, which is consistent with Eq. (4), since the subthreshold swing is also known to be linearly dependent on the interface trap density.[28,40]

The average value of S across all the TFTs is observed to increase from ~0.20 V/decade, prior to irradiation, to ~0.25 V/decade after 250 Gy, and finally to ~0.45 V/decade after 1000 Gy. Such changes should not significantly affect the addressing of AMFPI pixels since TFT switches are only operated in their conducting and nonconducting states. However, the change in S observed at the highest doses could conceivably cause performance problems in the case of the more complex circuits of in-pixel amplifiers, where TFTs may be operated in the subthreshold region.

D. Effects on leakage current

A problem commonly encountered with TFTs used as addressing switches is a dramatic increase in leakage current as a result of radiation. In the present study, both the shape and the magnitude of the transfer characteristics in the nonconducting region were found to undergo significant changes with increasing dose. Given the complexity of these changes, a relatively simple measure of the effect of radiation on leakage current for a given TFT was chosen based on how the magnitude of the minimum leakage current varied as a function of dose. This measure also facilitated meaningful comparisons between the various transistors (which exhibited leakage current minima at different negative gate voltages). The uncertainty in the measurement of this current is ~10% due to its very small magnitude. Figure 6 shows the leakage current of each of the eight TFTs as a function of dose, for a fixed source-drain voltage V_D of 5 V. This parameter is

associated with radiation-generated holes trapped in the gate oxide reduces the external electrical field needed to turn on the TFT,

$$\Delta V_{ot} = -q\Delta N_{ot}/C_{ox}, \tag{7}$$

where ΔN_{ot} is the increase in the aerial density of holes trapped in the gate oxide. Using Eqs. (4)–(7) along with the V_T data shown in Fig. 4(a), ΔV_T, ΔV_{it}, and ΔV_{ot} were determined and are plotted in Fig. 4(b). As seen in the figure, for the first ~500 Gy, the threshold voltage drops due to the dominance of ΔV_{ot}. Thereafter, ΔV_T slowly increases as a result of saturation in ΔV_{ot} and continued increases in ΔV_{it}. The sublinear changes in ΔV_{ot} (and ΔN_{ot}) of the poly-Si TFTs with increasing dose, followed by saturation, are also generally observed in the radiation response of *c*-Si MOS devices—although the dose level at which ΔN_{ot} saturates varies considerably for different devices.[38] Such saturation has been attributed to the fact that, as trapped charge builds up, the electric field in the gate oxide approaches zero and radiation-generated electron-hole pairs recombine more easily.[39]
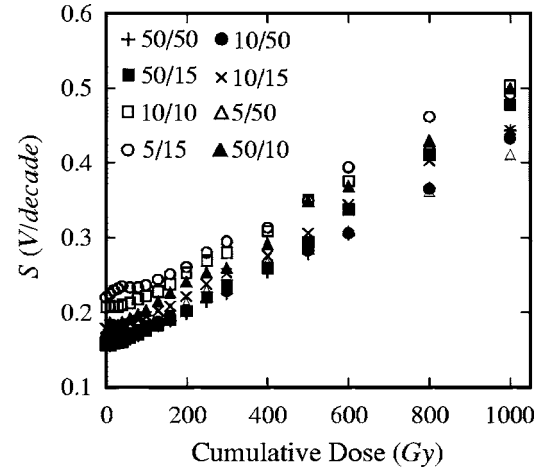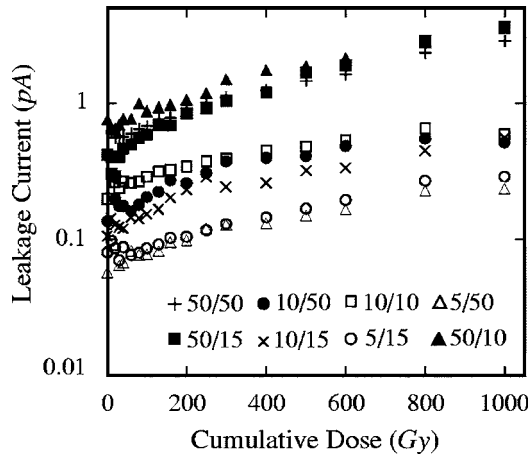
FIG. 6. Leakage current (corresponding to the minimum of the source-drain current in the nonconducting region of the transfer characteristics) as a function of dose.

found to increase by a factor of 1.6–2.4 after 250 Gy and by a factor of 3.0–8.7 after 1000 Gy. The increase in leakage current may be due to radiation-generated defects in the drain-depletion region. It has been found that the dominant mechanism of poly-Si TFT leakage current is thermionic-field emission,[41] and radiation-generated defects in the depletion region greatly reduce the potential barriers to electrons transported through this mechanism.[42]

It should be noted that the measured values of leakage current for these TFTs are sufficiently high, even before irradiation, so as to prohibit practical operation of an AMFPI based on the use of such TFTs as addressing switches. For

example, for an imager with a pixel charge capacity of 1 pC and a frame time of 1 s, good performance would preclude leakage currents in excess of ~0.1 pA. However, with the implementation of a small channel width (~10 μm) with a dual gate structure, more practical leakage currents (as low as 15 fA at V_D=5 V) can be obtained.[8] Furthermore, in the actual operation of an AMFPI, the source-drain voltage across addressing TFTs is typically much less than 5 V, resulting in even lower leakage current values. Therefore, it should be possible to configure poly-Si TFTs as addressing switches and keep the amplitude of the leakage current within the required range throughout the lifetime of AMPFI imagers.

E. Effects on source-drain current noise

While the TFT transfer characteristics directly determine the operation of AMFPIs, the TFT noise power spectrum is an important determinant of their signal-to-noise properties.[12] The noise power spectrum was determined for four TFTs by taking the square of the Fourier transform of the measured TFT source-drain current at a positive gate voltage of 15 V. For each TFT, the current was passed through a 10 kHz low-pass filter and sampled at 40 kHz. Noise power spectra obtained after 1000 Gy are shown in Fig. 7(a). These results are essentially identical to those obtained prior to the irradiation (not plotted). The TFT noise consists of two components; flicker noise S_f which dominates the low frequency spectrum and frequency-independent thermal noise S_t which dominates the high frequency spectrum. These components can be expressed as[43]
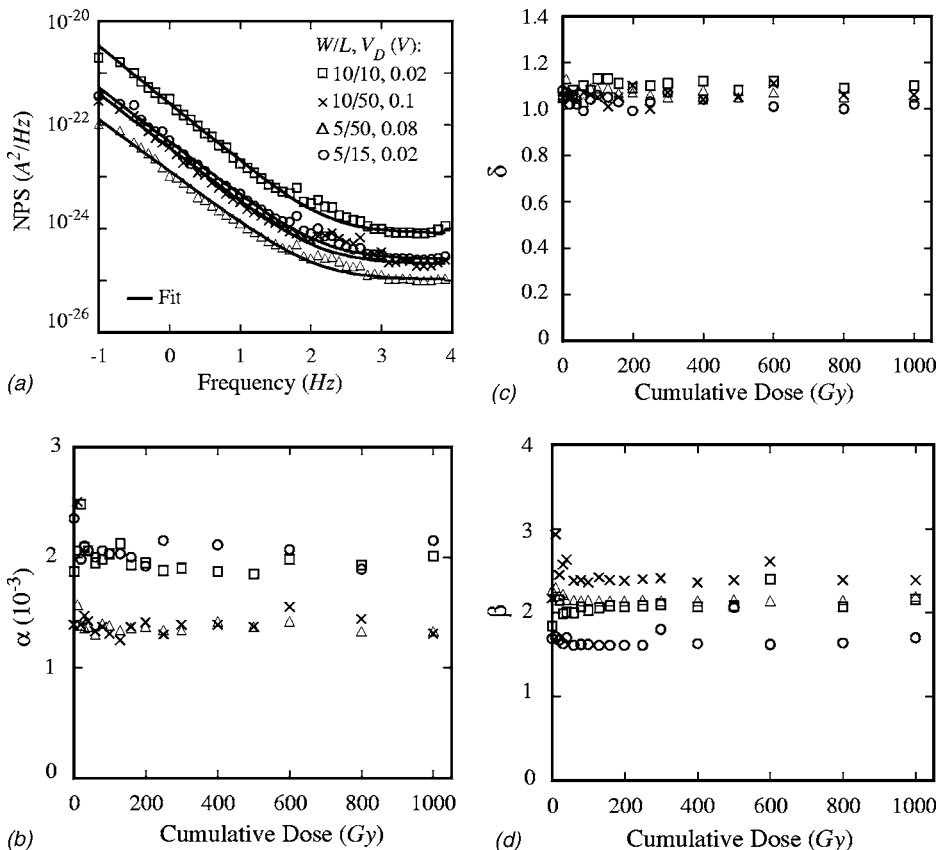

FIG. 7. (a) Noise power spectra of TFT source-drain current for four TFTs operated at different V_D values after 1000 Gy. The lines correspond to fits based on Eqs. (8) and (9). Coefficients derived from noise power spectra such as those of plotted as a function of dose, (b) flicker noise amplitude α, (c) flicker noise power spectrum coefficient δ, and (d) thermal noise amplitude β.

$$S_f(f) = \frac{\alpha q \mu^2 C_{ox}(W/L)^2}{(WL)f^\delta}\left(V_G - V_T - \frac{V_D}{2}\right)V_D^2, \quad (8)$$

$$S_t = 4\beta k T \mu C_{ox}(W/L)(V_G - V_T), \quad (9)$$

where f is the frequency, k is the Boltzmann constant, T is the temperature (295 K), and α, δ, and β are unitless coefficients. The coefficients α, δ, and β were obtained from fitting power spectra such as those shown in Fig. 7(a), and are plotted as a function of dose in Figs. 7(b)–7(d). No clear evidence of a radiation-induced change is observed in these coefficients, implying that noise properties of poly-Si TFTs are not affected by irradiations up to 1000 Gy.

IV. DISCUSSION

A. Charge trapped at the grain boundaries

The use of Eq. (2) in the above analysis is based upon the assumption that the mechanisms responsible for mobility degradation in poly-Si TFTs are the same as for c-Si TFTs. However, a complete understanding requires consideration of the unique structure of poly-Si thin films, which, in the analysis of transport properties, have been modeled as one-dimensional chains of crystalline grains with an amorphous interface.[44–46] Based on the idea that conduction in poly-Si TFTs is largely determined by thermionic emission across grain boundaries,[44–48] the current density J across a grain boundary can be written as[47]

$$J = qn\frac{\nu_r}{1 + \nu_r/\nu_d}e^{-qV_{pb}/kT}(e^{q\Delta V_{gb}/kT} - 1). \quad (10)$$

In this expression, n is the carrier density, ν_r is the velocity of thermal recombination at the grain boundary, ν_d is the velocity of drift diffusion within the grain, V_{pb} is the height of the potential barrier at the grain boundary, and ΔV_{gb} is the voltage drop across a grain boundary. For intrinsic poly-Si channels under sufficiently positive gate bias, V_{pb} can be expressed as[46]

$$V_{pb} = \frac{q^2 N_{bt}^2 t}{8\varepsilon C_{ox}(V_G - V_T)}, \quad (11)$$

where N_{bt} is the aerial density of trapping states at grain boundaries, t is the thickness of the poly-Si film (equal to ~50 nm in the present case), and ε is the permittivity of silicon. Integrating Eq. (10) over the cross section of a poly-Si channel, the following expression for the source-drain current I_D is obtained:

$$I_D = WC_{ox}(V_G$$
$$- V_T)\frac{\nu_r}{1 + \nu_r/\nu_d}e^{-q^3 N_{bt}^2 t/8\varepsilon C_{ox}(V_G - V_T)kT}(e^{q\Delta V_{gb}/kT} - 1).$$
$$(12)$$

Using this equation, and assuming that there is no strong dependence of ΔV_{gb} on V_G, N_{bt} can be determined from the slope of a linear fit of $\ln[I_D/(V_G - V_T)]$ plotted as a function of $1/(V_G - V_T)$.[46] Examples of such fits are shown in Fig. 8(a). Values for N_{bt} obtained in this manner, along with values for ΔN_{it} and ΔN_{ot} independently obtained from Eqs. (4)
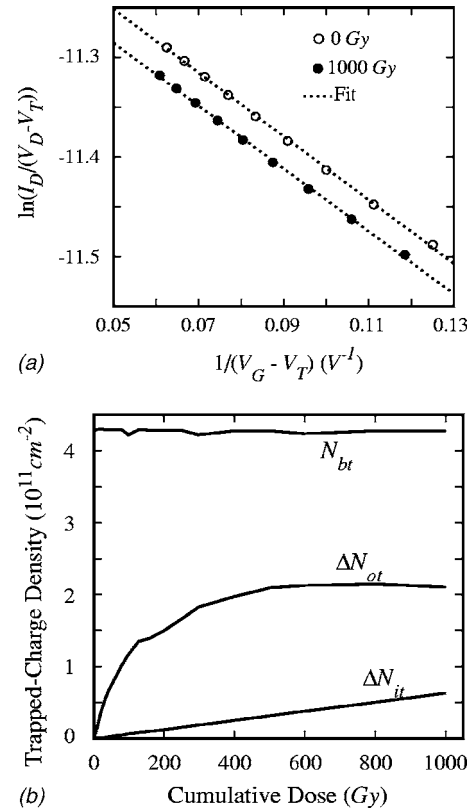

(a)

(b)

FIG. 8. (a) Plot of $\ln[I_D/(V_G - V_T)]$ as a function of $1/(V_G - V_T)$. The results shown correspond to data obtained from a TFT with $W=L=50$ μm prior to irradiation, and after receiving 1000 Gy. The dotted lines are linear fits obtained using Eq. (12), and N_{bt} is determined from the slope of these fits. (b) Aerial density of trapping states at the grain boundaries N_{bt} radiation-induced increase in holes trapped in the gate oxide ΔN_{ot}, and radiation-induced increase in the trapping states at the Si–SiO$_2$ interface ΔN_{it}.

and (7), respectively, were averaged over the eight TFTs and the results are plotted in Fig. 8(b) as a function of dose. N_{bt} is observed to remain at a constant value of ~4.3 $\times 10^{11}$ cm^{-2} over doses up to 1000 Gy, while ΔN_{it} and ΔN_{ot} exhibit dependence on dose. In principle, changes in either the density of trapping states at the grain boundaries or at the Si–SiO$_2$ interface would lead to changes in poly-Si TFT mobility. (It has been shown that changes in the density of trapping states in the gate oxide does not affect TFT mobility.[29]) The absence of significant changes in N_{bt} therefore implies that the observed mobility changes are due to changes in trapping state density at the Si–SiO$_2$ interface—thus supporting the assumption of the applicability of Eq. (2) to poly-Si TFTs in the present study.

B. Comparison with the behavior of *a*-Si and SPC poly-Si TFTs

In general, the measured effects of radiation on ELA poly-Si TFTs in the present study are more significant than effects observed in earlier studies on SPC poly-Si TFTs[25] and a-Si TFTs.[21] For example, 4%–5% reductions in mobility were found for the ELA poly-Si TFTs after ~1 kGy, while similar percentage reductions were observed for SPC poly-Si and a-Si TFTs only after receiving much higher doses (several kilograys and more than 20 kGy, respectively).

V. CONCLUSION

High levels of x-ray irradiation have been found to induce two major effects in ELA poly-Si TFTs: the creation of additional trapping states at the Si−SiO$_2$ interface and additional holes in the gate oxide. The density of trapping states at the interface increases linearly with cumulative dose up to 1000 Gy, leading to a degradation in the subthreshold swing from ~0.20 to ~0.45 V/decade, and to a degradation in mobility of ~5%. The density of holes trapped in the oxide is found to increase in a sublinear manner with cumulative dose until saturating at ~500 Gy. As a result of the combination of these two radiation-induced effects, the threshold voltage is found to shift toward negative voltages for the first ~500 Gy (where the effect of holes trapped in the oxide dominates), and slowly shifts toward positive voltages thereafter (where the effect of electrons trapped at the interface dominates). In addition, the density of trapping states at the grain boundaries was not found to be affected by the irradiation. Finally, no significant change is observed in either the flicker or thermal noise of the TFT source-drain current. The results of these initial studies are encouraging. They suggest that the effects of radiation on poly-Si TFTs are sufficiently small that the performance of AMFPIs incorporating such transistors for addressing and for more complex circuits (such as in-pixel amplifiers) should not be significantly affected at the dose levels associated with diagnostic imaging applications such as radiography, fluoroscopy, and mammography. However, for applications with higher levels of dose, such as radiotherapy, a higher degree of radiation tolerance would be desirable.

ACKNOWLEDGMENTS

[1] T. Kamins, *Polycrystalline Silicon for Integrated Circuits and Displays* (Kluwer Academic, Boston, 1998).
[2] H. Kuriyama *et al.*, IEEE Trans. Electron Devices **45**, 2483 (1998).
[3] R. K. Watts and J. T. C. Lee, IEEE Electron Device Lett. **14**, 515 (1993).
[4] T. Yamanaka *et al.*, Tech. Dig. - Int. Electron Devices Meet. 1988, 48.
[5] J. M. Wilson, R. Bashirullah, D. P. Nackashi, D. A. Winick, and P. D. Franzon, Proc. SPIE **5836**, 138 (2005).
[6] K. Yamamoto, M. Yoshimi, Y. Tawada, Y. Okamoto, A. Nakajima, and S. Igari, Appl. Phys. A: Mater. Sci. Process. **69**, 179 (1999).
[7] M. G. Clark, IEE Proc.: Circuits Devices Syst. **141**, 3 (1994).
[8] J. B. Boyce, R. T. Fulks, J. Ho, J. P. Lu, P. Mei, R. A. Street, K. F. van Schuylenbergh, and Y. Wang, Mater. Res. Soc. Symp. Proc. **609**, A31.4.1 (2000).
[9] S. D. Brotherton, Semicond. Sci. Technol. **10**, 721 (1995).
[10] L. E. Antonuk, Y. El-Mohri, K.-W. Jee, Q. Zhao, A. Sawant, Z. Su, and R. A. Street, Proc. SPIE **4682**, 1 (2002).
[11] L. E. Antonuk, in *Thin Film Transistors, Materials and Processes: Amorphous Silicon Thin Film Transistors*, edited by Y. Kuo (Kluwer Academic, Boston, 2004), Vol. 1, pp. 395–484.
[12] L. E. Antonuk *et al.*, Med. Phys. **27**, 289 (2000).
[13] Y. El-Mohri *et al.*, Proc. SPIE **5030**, 168 (2003).
[14] L. E. Antonuk *et al.*, Proc. SPIE **5745**, 18 (2005).
[15] K. S. Karim and A. Nathan, IEEE Electron Device Lett. **22**, 469 (2001).
[16] K. S. Karim, A. Nathan, and J. A. Rowlands, Digest IEDM '02, 2002, p. 215.
[17] J. B. Boyce, J. P. Lu, J. Ho, R. A. Street, K. Van Schuylenbergh, and Y. Wang, J. Non-Cryst. Solids **299–302**, 731 (2002).
[18] J. P. Lu, K. Van Schuylenbergh, J. Ho, Y. Wang, J. B. Boyce, and R. A. Street, Appl. Phys. Lett. **80**, 4656 (2002).
[19] R. A. Street, J.-P. Lu, and S. R. Ready, IEE Proc.: Circuits Devices Syst. **150**, 250 (2003).
[20] J. M. Boone, D. E. Pfeiffer, K. J. Strauss, R. P. Rossi, P.-J. P. Lin, J. S. Shepard, and B. J. Conway, Med. Phys. **20**, 789 (1993).
[21] J. M. Boudry, Thesis, University of Michigan, 1996.
[22] W. Zhao, D. Waechter, and J. A. Rowlands, Med. Phys. **25**, 527 (1998).
[23] M. Chevalier, P. Moran, J. I. Ten, J. M. F. Soto, T. Cepeda, and E. Vano, Med. Phys. **31**, 2471 (2004).
[24] This estimation is based on internal records at our institution in the past three years.
[25] C. K. Yang, C. L. Lee, T. F. Lei, and H. N. Chern, Appl. Phys. Lett. **67**, 3477 (1995).
[26] R. A. Street, *Technology and Applications of Amorphous Silicon* (Springer, New York, 2000).
[27] R. A. Street, *Hydrogenated Amorphous Silicon* (Cambridge University Press, Cambridge, New York, 1991).
[28] S. M. Sze, *Physics of Semiconductor Devices*, 2nd ed. (Wiley, New York, 1981).
[29] S. C. Sun and J. D. Plummer, IEEE Trans. Electron Devices **27**, 1497 (1980).
[30] F. B. McLean, IEEE Trans. Nucl. Sci. **27**, 1651 (1980).
[31] C. L. Wilson and J. L. Blue, IEEE Trans. Nucl. Sci. **31**, 1448 (1984).
[32] A. H. Johnston, IEEE Trans. Nucl. Sci. **31**, 1427 (1984).
[33] C. M. Dozier, D. B. Brown, J. L. Throckmorton, and D. I. Ma, IEEE Trans. Nucl. Sci. **32**, 4363 (1985).
[34] R. A. Kjar and D. K. DNichols, IEEE Trans. Nucl. Sci. **22**, 2193 (1975).
[35] L. E. Antonuk, J. Boudry, W. Huang, D. L. McShan, E. J. Morton, J. Yorkston, M. J. Longo, and R. A. Street, Med. Phys. **19**, 1455 (1992).
[36] P. J. McWhorter and P. S. Winokur, Appl. Phys. Lett. **48**, 133 (1986).
[37] K. F. Galloway, C. L. Wilson, and L. C. Witte, IEEE Trans. Nucl. Sci. **NS-32**, 4461 (1985).
[38] T. P. Ma and P. V. Dressendorfer, *Ionizing Radiation Effects in MOS Devices and Circuits* (Wiley, New York, 1989).
[39] H. E. J. Boesch, F. B. McLean, J. M. Benedetto, and J. M. McGarrity, IEEE Trans. Nucl. Sci. **33**, 1191 (1986).
[40] F. W. Sexton and J. R. Schwank, IEEE Trans. Nucl. Sci. **32**, 3975 (1985).
[41] I.-W. Wu, A. G. Lewis, T.-Y. Huang, W. B. Jackson, and A. Chiang, Tech. Dig. - Int. Electron Devices Meet. 1990, 867.
[42] W. B. Jackson, R. J. Nemanich, M. J. Thompson, and B. Wacker, Phys. Rev. B **33**, 6936 (1986).
[43] J. M. Boudry and L. E. Antonuk, J. Appl. Phys. **76**, 2529 (1994).
[44] J. Y. W. Seto, J. Appl. Phys. **46**, 5247 (1975).
[45] G. Baccarani, B. Ricco, and G. Spadini, J. Appl. Phys. **49**, 5565 (1978).
[46] J. Levinson, F. R. Shepherd, P. J. Scanlon, W. D. Westwood, G. Este, and M. Rider, J. Appl. Phys. **53**, 1193 (1982).
[47] P. V. Evans and S. F. Nelson, J. Appl. Phys. **69**, 3605 (1991).
[48] H. Ikeda, J. Appl. Phys. **91**, 4637 (2002).